

## Bose-Einstein correlations at LHCb

M. KUCHARCZYK on behalf of the LHCb Collaboration

*Henryk Niewodniczanski Institute of Nuclear Physics PAN - Krakow, Poland*

received 23 July 2024

**Summary.** — LHCb detector, considered as a general purpose detector in the forward rapidity region ( $2 < \eta < 5$ ), has a potential to investigate the quantum interference effects at large rapidities and low transverse momenta. The results on the Bose-Einstein correlations of same-sign charged pions are summarized, being measured in proton-proton collisions at  $\sqrt{s} = 7$  TeV centre-of-mass energy and proton-lead collisions at a nucleon-nucleon centre-of-mass energy of  $\sqrt{s_{NN}} = 5.02$  TeV. Both measurements are the first of this type performed in the forward region at LHC energies. Correlation parameters are determined for different regions of charged-particle multiplicity, which behaviour is consistent with observations from other experiments at the LHC in the central rapidity region. The measured correlation radii scale linearly with the cube root of the charged-particle multiplicity, being compatible with predictions based on the hydrodynamic models. The hints for a dependence of the correlation radius on pseudorapidity may also be observed.

### 1. – Introduction

The LHCb detector [1] is a single-arm spectrometer, equipped with a high-precision tracking and particle identification systems. Full instrumentation in the forward rapidity region  $2 < \eta < 5$ , with the efficient track and vertex reconstruction and very good particle identification at low angles with respect to the beam direction, provides an unique potential to investigate QCD effects in the forward region. The high precision results at the highest available collision energies obtained at LHCb are complementary to other LHC experiments with the coverage of the central rapidity region. The present document summarizes the first LHCb results on the Bose-Einstein correlations for same-sign charged pions originating from proton-proton [2] and proton-lead [3] collisions collected at  $\sqrt{s} = 7$  TeV centre-of-mass energy and  $\sqrt{s_{NN}} = 5.02$  TeV centre-of-mass energy per nucleon, respectively. The proton-proton (proton-lead) dataset used in the analysis was collected in 2011 (2013) and corresponds to an integrated luminosity of  $1.0 \text{ fb}^{-1}$  ( $1.6 \text{ nb}^{-1}$ ). The so-called small systems, *e.g.*, proton-proton and proton-lead collisions, characterized by significantly shorter lifetimes than the heavy-ion systems, may provide a better experimental insight into the early system dynamics and initial geometry [4, 5]. Thus, the present results make an important contribution to the understanding of the

particle production process in the forward direction at LHC energies as well as are an exclusive input to the development of the theoretical models. Moreover, a direct comparison of the results obtained by a single experiment in two different systems allows to establish a strong reference on the potential variations between the proton-proton and proton-lead collisions.

## 2. – Bose-Einstein correlations for pion pairs in proton-proton collisions at $\sqrt{s} = 7$ TeV

The study of the Bose-Einstein correlations (BEC) between two same-sign charged pions is based on the sample of proton-proton collisions collected at 7 TeV [2]. It relies on the measurement of the two-particle correlation function  $C_2(Q)$  [6] of indistinguishable pions with a small four-momenta difference  $Q$  [7], emitted by a finite-size source, being sensitive to the dynamic processes related to the evolution of the hadron source. The two-particle four-momenta difference is defined as  $Q = \sqrt{-(q_1 - q_2)^2} = \sqrt{M^2 - 4\mu^2}$ , where  $M$  is the invariant mass of the pair of particles and  $\mu$  denotes particle's rest mass. The correlations originate from the effects of quantum statistics as well as the strong and Coulomb final state interactions. In the case of particle physics, the Hanbury Brown-Twiss (HBT) interference effect [8], known from radioastronomy, manifests itself in the Bose-Einstein correlations between identical bosons, or Fermi-Dirac correlations in the case of fermions. The resulting correlations can provide information on the geometry of the particle source at a femtometer scale. The present analysis is based on the assumption of static, spherically-symmetric sources that can be characterized by univariate distributions. Therefore, the correlation function measures directly the absolute value of the Fourier transform of the source spatial distribution [9].

The correlation function is defined as a ratio of the inclusive density distribution for two identical particles and the reference density, which is a two-particle distribution without the BEC effect. In the present analysis a data-driven event-mixed reference sample is used, where the pions originate from different events, so the pairs naturally do not contain quantum interference effects. The correlation function is commonly parameterized as the so-called symmetric Lévy-stable distribution [10]. In the case of static, univariate sources, this parameterization has a following form:

$$(1) \quad C_2(Q) = N \cdot (1 + \lambda \cdot e^{-|RQ|^{\alpha_L}}) \cdot (1 + \delta \cdot Q),$$

where  $R$ , the correlation radius, can be interpreted as the radius of the spherically symmetric source of the emission volume,  $N$  accounts for the overall normalisation, and  $\lambda$  is the intercept parameter, which accounts for the partial incoherence of the source. Parameter  $\lambda$  can vary from zero, in the case of a completely coherent source, to unity for an entirely chaotic source. The  $\delta$  parameter accounts for long-range correlations, *e.g.*, related to the transverse momentum conservation, and  $\alpha_L$  is a parameter that can take values in the range  $0 < \alpha_L < 2$  and is referred to as a Lévy index of stability. Frequently, to enable comparison of the correlation parameters between experiments and between different collision systems,  $\alpha_L$  is fixed to unity, leading to the simplified expression:

$$(2) \quad C_2(Q) = N \cdot (1 + \lambda \cdot e^{-|RQ|}) \cdot (1 + \delta \cdot Q).$$

By construction of the correlation function, the effects due to single-particle efficiency, detector occupancy, acceptance and material budget are accounted for by dividing the

$Q$  distribution for same-sign charged pion pairs and a reference distribution. In order to account for the imperfections in the construction of the reference distribution as well as the effects related to the nonfemtoscopic background, in the present analysis the correlation function is improved by calculating a double ratio, defined as a ratio of the correlation function in the data constructed using the event-mixed reference sample and the correlation function in the simulation without the quantum interference effects, using an event-mixed sample built with simulated events in the same way as for data. The final state interactions involving both electromagnetic (Coulomb) and strong forces, are present in the Bose-Einstein correlation region and may potentially affect the distributions of analysed observables. Strong final state interactions are present in both charged and neutral hadron systems, while the Coulomb interactions exert an influence only on the charged hadron systems. The effect of the strong interactions in the case of pions is relatively small and is usually neglected in BEC studies. A correction for the Coulomb interactions between the same-sign charged particles was performed using the Gamov penetration factor [11]:

$$(3) \quad K_{Gamov}(\zeta) = \frac{2\pi\zeta}{e^{2\pi\zeta} - 1},$$

where  $\zeta = \alpha m / Q$ ,  $\alpha$  is the fine-structure constant and  $m$  is the particle rest mass. It was possible to use this simplification because of the small size of the pion source that can be treated more as a point-like. As the correlation parameters are expected to be dependent upon the particle multiplicity, Bose-Einstein correlations are studied in different bins of reconstructed charged-particle multiplicity. Activity classes are introduced, better reflecting the total multiplicity in the full solid angle. Activity bins were related to the fractions of multiplicity of charged-particles reconstructed in the vertex detector, which is a good analogue of the total multiplicity.

The dependence of the correlation radius and intercept parameter on event activity has been investigated in the present analysis in the forward acceptance region of  $2 < \eta < 5$  for single pions with transverse momentum  $p_T > 0.1$  GeV/c. First, the Coulomb corrected double ratios in three different activity bins were fitted with the Lévy parameterization from eq. (2), where an enhancement related to the BEC effect on the double ratio distributions for pairs of same-sign charged pions might be observed in the region of low relative momentum. Figure 1 shows the dependence of the Bose-Einstein correlation parameters on event activity, where the correlation radius increases with event activity, while the intercept parameter is decreasing. The dominant contribution to the systematic uncertainty is due to differences in the event generators used to construct the double ratio as well as pile-up effects. The trends observed agree well with the previous dependencies measured at LEP and other LHC experiments [12].

### 3. – Bose-Einstein correlations for pion pairs in proton-lead collisions

The measurement of the two-particle Bose-Einstein correlations for same-sign charged pions have been performed at LHCb in  $p$ Pb collisions at  $\sqrt{s_{NN}} = 5.02$  TeV [3]. The data was collected in 2013 in two beam modes, *i.e.*,  $p$ Pb, with the proton beam along the LHCb detector (towards positive values on the  $z$ -axis in the LHCb coordinate system), and Pb $p$ , with opposite directions of the beams. As the  $p$ Pb collisions are asymmetric, there is a shift of  $\sim 0.465$  between pseudorapidities measured in the LHCb laboratory frame and in the nucleon-nucleon centre-of-mass system. This allows to examine the  $p$ Pb

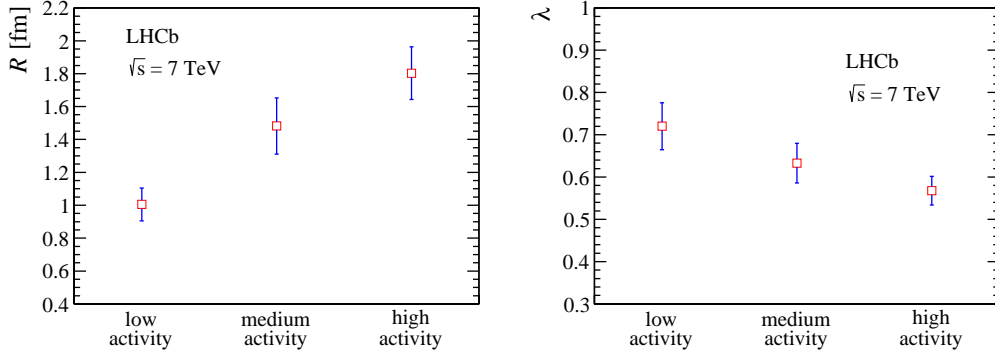


Fig. 1. – Correlation radius  $R$  (left) and intercept parameter  $\lambda$  (right) as a function of activity. Error bars indicate the sum in quadrature of the statistical and systematic uncertainties. The points are placed at the centres of the activity bins. Figure adopted from [2].

system in the forward ( $1.5 < \eta < 4.5$ ) and backward ( $-5.5 < \eta < -2.5$ ) directions. The analysis uses a data-driven event-mixed reference sample and it is performed in common bins of multiplicity of charged-particles reconstructed in the vertex detector ( $N_{\text{VELO}}$ ), allowing a direct comparison between the two beam configurations. Moreover, this gives an opportunity to investigate a potential dependence of the measured BEC parameters on pseudorapidity. The results are interpreted within the frame of hydrodynamic models.

In the present analysis the correlation function is parameterized employing a Bowler-Sinyukov formalism [13, 14], which allows to properly introduce Coulomb interactions as well as the nonfemtoscopic background in the experimentally measurable correlation function. A full parameterization of the correlation function is defined as:

$$(4) \quad C_2(Q) = N \left[ 1 - \lambda + \lambda K(Q) \times \left( 1 + e^{-|RQ|} \right) \right] \times \Omega(Q),$$

where  $N$  is a normalisation factor and  $\Omega(Q)$  denotes a general term for the nonfemtoscopic background.

It uses the general  $K(Q)$  term for the Coulomb effect for extended sources [13]. Opposite to the point-like sources where the Gamov factor is used to correct for the Coulomb interactions, calculating  $K(Q)$  in its full form for extended sources is time-consuming and requires a numerical, iterative approach. This is why a parameterization of the  $K(Q)$  term developed by the CMS experiment and valid for Lévy sources with  $\alpha_L = 1$  is used in the present analysis [15]:

$$(5) \quad K(Q) = K_{\text{Gamov}}(Q) \left( 1 + \frac{\alpha \pi m R_{eff}}{1.26 + QR_{eff}} \right),$$

where  $R_{eff}$  corresponds to the effective size of the particle source and is provided in femtometers. The additional term with  $R_{Eff}$  constitutes a correction for the Gamov factor, allowing a more precise characterization of the Coulomb effect for extended sources.

The major input to the nonfemtoscopic background is referred to as cluster contribution [15, 16]) including effects related to the minijets fragmentation and multibody

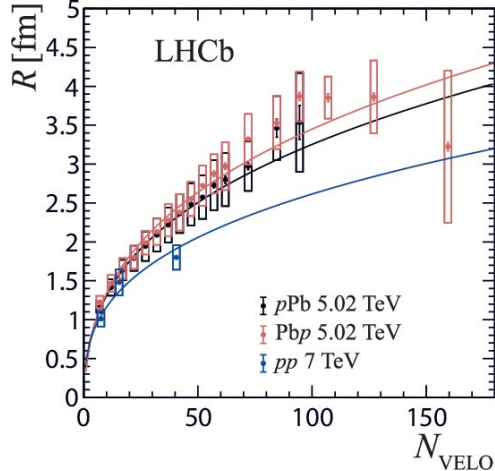


Fig. 2. – Correlation radius as a function of  $N_{\text{VELO}}$  measured in the  $pp$  [2] and  $p\text{Pb}$  (Pbp) [3] collision systems. Error bars denote the statistical uncertainties, while boxes illustrate the systematic ones. Data points are positioned at the centres of the multiplicity bins. Results of the fits to the correlation radii as a function of the reconstructed multiplicity as described in the text are indicated by the solid lines. Figure adopted from [3].

resonance decays, as they are most prominent in the low- $Q$  region and may overlap with the BEC signal. It was found that it can be properly parameterized using relatively simple parametrizations, like for example a Gaussian function [15-17]). Such effects are studied using a cluster subtraction method developed by the CMS experiment [15, 16], and are parameterized with the correlation functions for opposite-sign pairs. This is a fully data-driven technique. Because of a presence of structures related to the two-body decays of resonances in the correlation functions for opposite-sign pairs, the affected regions are removed from the fit to the correlation function.

As the bin contents in both the signal and reference  $Q$  distributions are Poisson-distributed, a negative log-likelihood fit method is used [18, 19]. In this kind of approach, the following expression is minimized during the fitting procedure:

$$(6) \quad -2 \ln L = 2 \sum_i \left\{ A_i \ln \left[ \frac{(1 + C_i) A_i}{C_i (A_i + B_i + 2)} \right] + (B_i + 2) \ln \left[ \frac{(1 + C_i) (B_i + 2)}{A_i + B_i + 2} \right] \right\},$$

where  $A_i$  and  $B_i$  are the bin contents of the signal and reference  $Q$  distributions, while  $C_i$  corresponds to the fit function value at the bin centre. Finally, such a negative log-likelihood function is constructed for all of the  $N_{\text{VELO}}$  bins in the given dataset and minimized globally to obtain the best description of the data.

The correlation parameters measured in a function of multiplicity of charged-particles reconstructed in the vertex detector for both  $p\text{Pb}$  and  $\text{Pbp}$  datasets are illustrated in figs. 2 and 3. The dominant contribution to the systematic uncertainty is due to the parameterization of nonfemtoscopic background in the correlation function, including also the effect related to the removal of the structures induced by two-body resonance decays from the fits to the correlation functions for opposite-sign pairs. They are compared

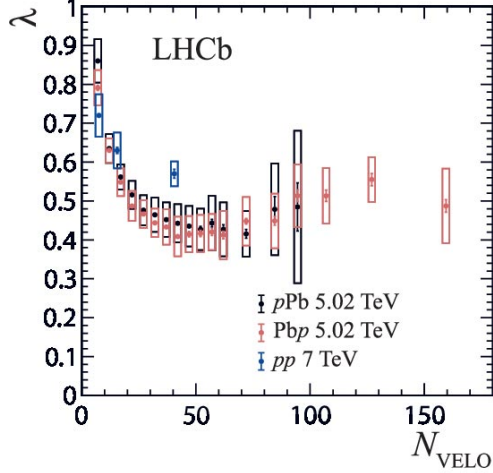


Fig. 3. – Intercept parameter as a function of  $N_{\text{VELO}}$  measured in the  $pp$  [2] and  $p\text{Pb}$  (Pb $p$ ) [3] collision systems. Error bars indicate the statistical uncertainties, while boxes illustrate the systematic ones. Data points are positioned at the centres of the multiplicity bins. Figure adopted from [3].

also with the correlation parameters determined in the BEC studies for the  $pp$  [2]. It may be observed that the measured correlation radii scale linearly with the cube root of the reconstructed charged-particle multiplicity. This kind of scaling was also reported by other experiments at LHC for various collision systems [16, 17, 19]. It is a behaviour compatible with predictions of hydrodynamic models on the system evolution [20-22]. It may be seen that the central  $R$  values in the Pb $p$  sample tend to be systematically higher as compared to the  $p\text{Pb}$  one, however, the results in both samples agree well within the systematic uncertainties. This could point to a behaviour similar to the one reported by the ATLAS experiment for  $p\text{Pb}$  collisions [19]. As the proton-lead system is investigated in both forward and backward directions, some hints for a potential sensitivity of the correlation parameters to the rapidity may be seen.

#### 4. – Conclusions

The LHCb experiment provides complementary results on particle correlations to the general purpose LHC detectors in the forward kinematic region. The Bose-Einstein correlations between two indistinguishable charged pions have been performed for the first time in the LHCb experiment with the  $pp$  and the  $p\text{Pb}$  collisions at  $\sqrt{s} = 7$  TeV centre-of-mass energy and  $\sqrt{s_{NN}} = 5.02$  TeV centre-of-mass energy per nucleon, respectively. Both  $pp$  and  $p\text{Pb}$  analyses use the event-mixing method for constructing the reference sample, and a Lévy-type parameterization of the correlation function with the index of stability fixed to unity. Two alternative approaches for the nonfemtoscopic background are used, *i.e.*, double-ratio for  $pp$  and a data-driven approach to parametrize the cluster contribution in the case of  $p\text{Pb}$ . The measured correlation radii scale linearly with a cube root of reconstructed charged-particle multiplicity, being compatible with predictions of hydrodynamic models on the system evolution. The  $p\text{Pb}$  system is investigated both in

the forward and backward direction due to asymmetric beams and hints for a potential sensitivity of the correlation radii to pseudorapidity may be observed.

## REFERENCES

- [1] LHCb COLLABORATION (AAIJ R. *et al.*), *Int. J. Mod. Phys.A*, **30** (2015) 1530022.
- [2] LHCb COLLABORATION (AAIJ R. *et al.*), *JHEP*, **12** (2017) 025.
- [3] LHCb COLLABORATION (AAIJ R. *et al.*), *JHEP*, **09** (2023) 172.
- [4] SCHENKE B. and VENUGOPALAN R., *Phys. Rev. Lett.*, **113** (2014) 10230.
- [5] ROMATSCHKE P., *Eur. Phys. J. C*, **75** (2015) 305.
- [6] LORSTAD B., *Int. J. Mod. Phys. A*, **4** (1989) 2861.
- [7] BAYM G., *Acta Phys. Pol. B*, **29** (1998) 1839.
- [8] BROWN R. H. and TWISS R. Q., *Phil. Mag.*, **45** (1954) 663.
- [9] KITTEL W., *Acta Phys. Pol. B*, **32** (2001) 3927.
- [10] CSORGO T., HEGYI S and ZAJC W.A., *Eur. Phys. J. C*, **36** (2004) 67.
- [11] PRATT S., *Phys. Rev. D*, **33** (1986) 72.
- [12] BUSCHBECK B., EGGERS H. C. and LIPA P., *Phys. Lett. B*, **481** (2000) 187.
- [13] BOWLER M. G., *Phys. Lett. B*, **270** (1991) 69.
- [14] SINYUKOV Y., *Phys. Lett. B*, **432** (1998) 248.
- [15] CMS COLLABORATION (SIRUNYAN A. M. *et al.*), *Phys. Rev. C*, **97** (2018) 064912.
- [16] CMS COLLABORATION (SIRUNYAN A. M. *et al.*), *JHEP*, **03** (2020) 014.
- [17] ALICE COLLABORATION (ADAM J. *et al.*), *Phys. Rev. C*, **91** (2015) 034906.
- [18] E802 COLLABORATION (AHLE L. *et al.*), *Phys. Rev. C*, **66** (2002) 054906.
- [19] ATLAS COLLABORATION (AABOUD M. *et al.*), *Phys. Rev. C*, **96** (2017) 064908.
- [20] WERNER K. *et al.*, *Phys. Rev. C*, **83** (2011) 044915.
- [21] BOZEK P. and BRONIEWSKI W., *Phys. Lett. B*, **720** (2013) 250.
- [22] SHAPOVAL V. M., BRAUN-MUNZINGER P., KARPENKO I. A. and SINYUKOV Y., *Phys. Lett. B*, **725** (2013) 139.